Experimental and Computational Investigation on the Gas Phase Reaction of p -Cymene with Cl Atoms

ARTICLE *in* THE JOURNAL OF PHYSICAL CHEMISTRY A · DECEMBER 2014

Impact Factor: 2.69 · DOI: 10.1021/jp509800g · Source: PubMed

3 AUTHORS, INCLUDING:

Manas Dash
National Chiao Tung University
10 PUBLICATIONS **44** CITATIONS
SEE PROFILE

Srinivasulu Gonu
Indian Institute of Technology Madras
3 PUBLICATIONS **11** CITATIONS
SEE PROFILE

THE JOURNAL OF PHYSICAL CHEMISTRY A

Article

pubs.acs.org/JPCA

Experimental and Computational Investigation on the Gas Phase Reaction of *p*-Cymene with Cl Atoms

Manas Ranjan Dash, G. Srinivasulu, and B. Rajakumar*

Department of Chemistry, Indian Institute of Technology Madras, Chennai 600036, India

Supporting Information

ABSTRACT: The rate coefficient for the gas-phase reaction of Cl atoms with *p*-cymene was determined as a function of temperature (288−350 K) and pressure (700−800 Torr) using the relative rate technique, with 1,3-butadiene and ethylene as reference compounds. Cl atoms were generated by UV photolysis of oxalyl chloride ($(COCl)_2$) at 254 nm, and nitrogen was used as the diluent gas. The rate coefficient for the reaction of Cl atoms with *p*-cymene at 298 K was measured to be $(2.58 \pm 1.55) \times 10^{-10}$ cm^3 molecule^{-1} s^{-1}. The kinetic data obtained over the temperature range 288−350 K were used to derive an Arrhenius expression: $k(T) = (9.36 \pm 2.90) \times 10^{-10} \exp[-(488 \pm 98)/T]$ cm^3 molecule^{-1} s^{-1}. Theoretical kinetic calculations were also performed for the title reaction using canonical variational transition state theory (CVT) with small curvature tunneling (SCT) between 250 and 400 K. The calculated rate coefficients obtained over the temperature range 250−400 K were used to derive an Arrhenius expression: $k(T) = 5.41 \times 10^{-13} \exp[1837/T]$ cm^3 molecule^{-1} s^{-1}. Theoretical study indicated that addition channels contribute maximum to the total reaction and H-abstraction channels can be neglected. The atmospheric lifetime (τ) of *p*-cymene due to its reactions with various tropospheric oxidants was estimated, and it was concluded that the reactions of *p*-cymene with Cl atoms may compete with OH radicals in the marine boundary layer and in coastal urban areas where the concentration of Cl atoms is high.

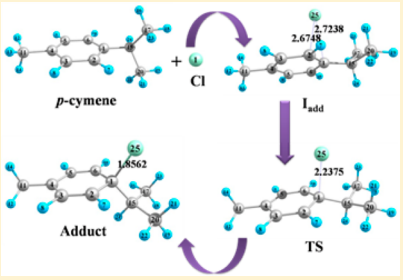

1. INTRODUCTION

Volatile organic compounds (VOCs) are emitted into the Earth's atmosphere from various anthropogenic and biogenic sources (generally known as biogenic volatile organic compounds (BVOCs)).[1−4] Globally, emissions of VOCs from the biogenic sources (mostly by vegetation) are estimated to dominate over anthropogenic sources.[1,5−8] Guenther et al.[1] have estimated that 1150 Tg C year^{-1} of VOCs are emitted from vegetation. Alkenes are dominated in all types of biogenic emissions, composed of 44% isoprene and 11% monoterpenes.[1] In the Earth's atmosphere, potential removal of these biogenic compounds mainly occurs by reactions with oxidizing agents such as OH and NO_3 radicals and O_3 molecules, which leads to the formation of a series of organic oxidation products. These products play an important role in the chemistry of the troposphere and are known to contribute significantly to the formation of secondary organic aerosols (SOAs) and tropospheric ozone.[5,8−13] Such organic aerosols are hazardous to health and may influence the cloud nucleation in the troposphere.[14−17] Chlorine atoms (Cl) can also play an important role in the oxidative capacity of the troposphere particularly in the early morning,[18] and its global concentration is about 10^3 atoms cm^{-3}.[19,20] Cl atoms generally react with BVOCs much faster than corresponding OH radical reactions. Moreover, in the marine boundary layer (MBL) and coastal regions, it is estimated that the Cl atom concentration is significantly higher, reaching a peak concentration of about 10^5 atoms cm^{-3}.[21] Therefore, reactions with chlorine atoms in those areas may represent a significant sink for BVOCs. The main source of chlorine atoms in the atmosphere is generally assumed to be the photolysis of chlorine containing compounds produced in the sea-salt aerosols.[21,22] Moreover, recent field studies observed that nitryl chloride ($ClNO_2$) is a gaseous photolytic Cl atom precursor[18,23,24] in continental regions and which is formed in the night-time reaction of N_2O_5 with chloride-containing aerosol.[25] The interaction between BVOCs with chlorine atoms might occur when sea breezes carry marine air masses inland, and in addition to this, some biogenic compounds are also expected to be emitted by the oceans.[26−30]

p-Cymene [1-methyl-4-(1-methylethyl) benzene or 4-isopropyltoluene] is a naturally occurring monoterpene emitted from vegetation.[31] Recently, Aschmann et al.[32] measured the molar formation yield of *p*-cymene from the γ-terpinene [1-methyl-4-(1-methylethyl)-1,4-cyclohexadiene] + OH reaction to be 13.6 ± 2.5%. To the best of our knowledge, several experimental and theoretical investigations on the reaction rate coefficients of OH radicals with *p*-cymene have been reported,[33−35] but only one kinetic study on the reaction of *p*-cymene with Cl atoms is available in the literature.[36] Finlayson-Pitts et al.[36] carried out the reaction of *p*-cymene with Cl atoms at 298 K and 1 atm pressure using a relative rate technique. The reported rate coefficient is $(2.1 \pm 0.4) \times 10^{-10}$ cm^3 molecule^{-1} s^{-1}. Temperature dependent rate coefficients

Received: September 28, 2014
Revised: December 27, 2014
Published: December 29, 2014

DOI: 10.1021/jp509800g
J. Phys. Chem. A 2015, 119, 559−570

for this reaction are lacking. In this work, the kinetics of the reaction of Cl atoms with *p*-cymene were studied for the first time as a function of temperature (288−350 K) by means of a relative rate technique. In addition, theoretical calculations on the title reaction were also carried out by using various *ab initio* methods to provide some additional insights into the energetics. The rate coefficients are also computed using canonical variational transition state theory (CVT) in combination with the small curvature tunneling (SCT) method in the temperature range 250−400 K. The data obtained in this work were used to estimate the effective lifetime of *p*-cymene in the troposphere.

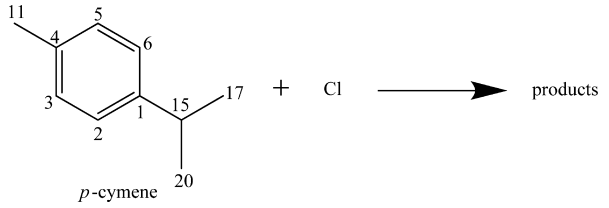

2. EXPERIMENTAL AND COMPUTATIONAL METHODS

2.1. Experimental Section. The experiments were carried out in two different types of reaction chambers. The room temperature experiments were carried out using 1,3-butadiene as a reference compound in a quartz reaction chamber of ∼1750 cm^3 volume at 298 K and ∼800 Torr of N_2. The details of the experimental setup are given elsewhere,[37,38] and only a brief description is given here. Cl atoms were produced by the photolysis of oxalyl choride ($(COCl)_2$) at 254 nm, using two UV lamps (SANKYO DENKI G8T5, 8 W).

$$(COCl)_2 + h\upsilon\ (\approx 254\ nm) \rightarrow 2Cl + 2CO$$

The reaction mixtures, consisting of *p*-cymene (reactant), 1,3-butadiene (reference compound), oxalyl chloride, and nitrogen, were prepared in the reaction chamber and kept for 30−45 min for equilibration before photolysis. The reaction mixtures were photolyzed for a period of 30 s, in steps of 10 s, and after each photolysis step, the decrease in the concentration of the reactant and reference compounds was determined, using a gas chromatograph (GC) (Agilent Technologies 6890N), with a capillary column (HP-5, 30 m × 0.320 mm × 0.25 μm, 19091J-413), in conjunction with a flame ionization detector. A sample of 500 μL was transferred from the reaction chamber (∼2 L volume) to GC, using a gastight syringe. The GC column was run at 75 °C oven temperature, 160 °C inlet temperature, and 170 °C detector temperature.

Temperature dependence reactions were carried out using ethylene as a reference compound in a double-walled Pyrex reaction chamber of ∼1250 cm^3 equipped with UV fused silica broadband precision windows at both ends. The details of the experimental setup are given elsewhere in our recently published articles.[39,40] The temperature in the reaction cell was maintained by circulating a cooled/heated fluid through the outer jacket. The temperature inside the reaction chamber was calibrated by using a K-type thermocouple within the uncertainty of 2 K. The title reaction was investigated over the pressure range 700−800 Torr of N_2/air and the temperature range 288−350 K. The reaction mixtures were photolyzed for 10−30 min. Both reaction chambers have different geometries. Therefore, the photolysis times for both reaction chambers are different. The GC conditions are the same for both the room temperature study and the temperature dependence study.

The initial concentration ranges used in the experiments were 4.5 × 10^{16} to 7 × 10^{16} molecules cm^{-3} for the reactants, 1.7 × 10^{15} to 3.7 × 10^{17} molecules cm^{-3} for the reference compounds, and 8.6 × 10^{16} to 1.2 × 10^{18} molecules cm^{-3} for $(COCl)_2$.

The kinetic data were obtained from the measurement of the simultaneous loss of reactant and reference compound, using the standard expression

$$\ln\left(\frac{[\text{reactant}]_0}{[\text{reactant}]_t}\right) = \left(\frac{k_{\text{reactant}}}{k_{\text{reference}}}\right)\ln\left(\frac{[\text{reference}]_0}{[\text{reference}]_t}\right) \quad (1)$$

where $[\text{reactant}]_0$ and $[\text{reference}]_0$ are the initial concentrations of reactant and reference compound and $[\text{reactant}]_t$ and $[\text{reference}]_t$ are the corresponding concentrations at time "*t*".

Few preliminary tests were performed to verify the decrease in the concentration of reactant and reference compounds are removed only because of their reaction with Cl atoms. The mixtures of reactant and reference compounds, $(COCl)_2$, and nitrogen were loaded in the reaction cell and allowed to mix in the absence of UV light for about 5 h, which is more than the total duration of a relative rate measurement. The concentrations of the reactant and reference compounds were monitored by GC at different time intervals. There was no significant decrease in concentration of any of the compounds, indicating the absence of any dark reaction as well as wall loss. We have also photolyzed the reaction mixture for 30 min in the absence of $(COCl)_2$ to ensure no significant decrease in the concentration of reactant and reference compounds. We did not observe any such decrease in the concentration of both of the compounds.

Chemicals. *p*-Cymene (purity 99%, Sigma-Aldrich), 1,3-butadiene (purity 99.5%, PRAXAIR), ethylene (purity 99.5%, PRAXAIR), oxalyl chloride (purity 98%, SPECTROCHEM), nitrogen (99.995%), zero air (98%), and oxygen (98%). *p*-Cymene and oxalyl chloride were subjected to repeated freeze−pump−thaw cycles before use.

2.2. Computational Methodology. All the electronic structure calculations were carried out using the Gaussian 09 program.[41] The geometries of the reactants, intermediates (I_{adds}), transition states (TSs), and products of all possible addition and abstraction channels were optimized at the MP2/6-31G(d), MP2/6-31G(d,p), MP2/6-31+G(d,p), MP2-(FULL)/6-31G(d), and MP2(FULL)/6-31+G(d,p) levels of theory. Single point calculations at the QCISD(T) and CCSD(T) levels were carried out by taking the optimized structures obtained at the above levels of theory, in order to obtain more reliable energy. The theoretical rate coefficients for the title reaction were computed using canonical variational transition state theory (CVT)[42−44] with small curvature tunneling (SCT)[45,46] by employing the POLYRATE 2008 program[47] and GAUSSRATE 2009A.[48]

$$k^{GT}(T, s) = \sigma\frac{k_B T}{h}\left(\frac{Q^{GT}(T, s)}{\Phi^R(T)}\right)\exp\left(\frac{-V_{MEP}(s)}{k_B T}\right) \quad (2)$$

$$k^{CVT}(T) = \min_s k^{GT}(T, s) = k^{GT}[T, s^{CVT}(T)] \quad (3)$$

where k^{GT} and k^{CVT} are the rate coefficients of the generalized and canonical variational transition state theories, respectively, σ is the reaction path degeneracy, k_B is Boltzmann's constant, *h*

DOI: 10.1021/jp509800g
J. Phys. Chem. A 2015, 119, 559−570

is Planck's constant, T is the temperature in Kelvin, and s^{CVT} is the reaction coordinate (s) at which the canonical variational transition state dividing surface was found. Q^{GT} and Φ^{R} are the partition functions of a generalized TS at "s" and reactants, respectively. $V_{MEP}(s)$ is the potential energy of a generalized TS at "s". The canonical variational transition state is located by maximizing the free energy of activation with respect to "s". The two spin−orbit (SO) states $^2P_{3/2}$ (lowest) and $^2P_{1/2}$ of Cl having degeneracies of 4 and 2, respectively, and separated by 882.3515 cm^{-1} were included in the Cl atom electronic partition function calculations.[49] The tunneling corrected rate coefficients were obtained by multiplying the CVT rate constant by a temperature-dependent transmission coefficient $\kappa^{CVT/SCT}(T)$

$$k^{CVT/SCT}(T) = \kappa^{CVT/SCT}(T)k^{CVT}(T) \quad (4)$$

3. RESULTS AND DISCUSSION

3.1. Experimental Section. Figure 1 shows the typical experimental plot derived from the analysis of relative rate

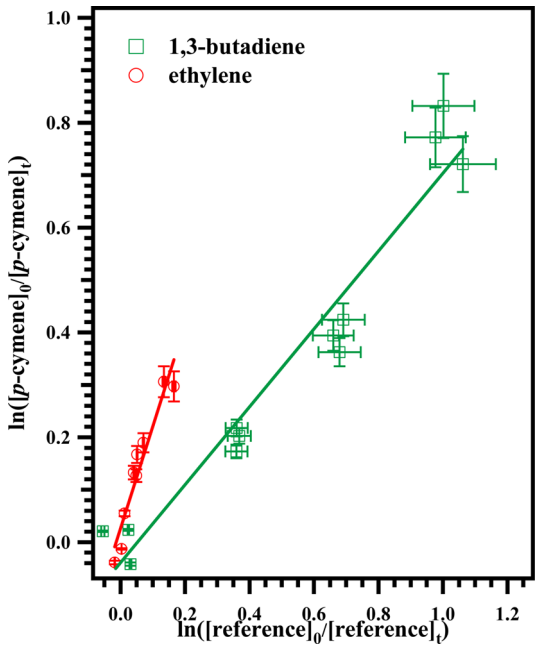

Figure 1. Plot of the relative decrease in the concentration of *p*-cymene due to its reaction with Cl atom at 298 K in N_2.

measurements at 298 K in N_2. As expected, a straight line with a zero intercept was obtained. The rate coefficient ratios ($k_{p\text{-cymene}}/k_{ref}$) and the obtained rate coefficients at 298 K are summarized in Table 1. For each experiment, the slope and errors were obtained from the linear least-squares fitting of the data. As seen in Table 1, the mean value of the slopes is $k_{p\text{-cymene}}/k_{1,3\text{-butadiene}} = 0.79 \pm 0.17$. From this slope, using $k_{1,3\text{-butadiene}} = (4.2 \pm 0.4) \times 10^{-10}$ cm^3 $molecule^{-1}$ s^{-1} [50] at 298 K, the rate coefficient of the *p*-cymene + Cl reaction was calculated to be $(3.30 \pm 0.78) \times 10^{-10}$ cm^3 $molecule^{-1}$ s^{-1} at 298 K. The quoted errors are two least-squares standard deviations and include uncertainties associated with the rate coefficient of $k_{1,3\text{-butadiene}}$.[50] The temperature dependence of the reaction of Cl atoms with *p*-cymene was investigated over the temperature range 288−350 K, using ethylene as a reference compound. Coquet and Ariya[51] studied the rate coefficients of Cl atoms with ethylene over the temperature range 283−323 K in air and N_2 at an atmospheric pressure of 760 Torr. Therefore, the rate coefficients as a function of temperature reported by Coquet and Ariya,[51] $k_{ethylene} = (0.39 \pm 0.22) \times 10^{-11}$ $\exp\{-(-7.9 \pm 1.5) \times 1000/RT\}$ cm^3 $molecule^{-1}$ s^{-1}, were used in the present experiments. This work represents the first kinetic study of the temperature dependence of the reactions of Cl atom with *p*-cymene. The relative rate coefficients were measured at 288, 298, 310, 325, 340, and 350 K, and the obtained rate coefficients are given in Table 1. Few experiments at room temperature and at the extreme ends of the studied temperatures (288 and 350 K) were carried out in air to see any significant influence of secondary reactions on the measured rate coefficients. We observed that the two bath gases produce identical results, which provide strong evidence of no significant influence of secondary reactions because of the presence of oxygen. Each set of experiments has been repeated at least twice. For each experiment, the slope and errors were obtained from the linear least-squares fitting of the data. The quoted errors for the rate coefficients are two least-squares standard deviations and include uncertainties associated with the rate coefficients of ethylene.[51] Oxalyl chloride and aromatic compounds have similar absorption cross sections at 254 nm. The excitation radiation used to photolyze the oxalyl chloride is 254 nm. It is well studied and established that this photolysis generates Cl in its ground state ($^2P_{3/2}$) in addition to few percent of excited state Cl ($^2P_{1/2}$).[52] The relaxation time of an excited state Cl atom in the inert environment is much faster than the reaction with any hydrocarbon.[53,54] In addition, quenching is more likely than the reaction with the hydrocarbons.[53,54] The excited state Cl atom reacts with hydrocarbons slower than the ground state chlorine atoms due to the absence of an adiabatic pathway.[54] Therefore, the contribution of reactions of excited states in the mixture (if any) is negligible in these studies. As far as the excitation of *p*-cymene in the wavelength region of 254 nm is considered, no studies are reported to the best of our knowledge. However, the contribution of the *p*-cymene in the excited state to the reaction may not be ruled out, although no significant depletion of *p*-cymene was observed in the absence of the oxalyl chloride. It can be seen from Table 1 that the experiments are performed at different initial concentrations of *p*-cymene, reference compounds, and oxalyl chloride and the obtained slopes are independent of these concentrations. Figure 2 shows typical plots of accumulated data for the reaction of Cl atoms with *p*-cymene at 298, 325, and 350 K in N_2. The little shift from the origin is the errors associated with the measurements of initial concentrations of both reactant and reference compounds. The reproducibility of the data was within 15%, except for the reaction at subambient temperature (288 K), where the lower vapor pressure of the *p*-cymene led to reproducibility of the data to be within 30%. The vapor pressures of *p*-cymene, 1,3-butadine, and ethylene are 1.5 mmHg, ~50 atm, and 2.5 atm at room temperature. It should be noted that, at 288 K, the vapor pressure of *p*-cymene is less than 1 mmHg. We have included the error limits ($\pm 2\sigma$) in Figures 1 and 2. For each point in Figures 1 and 2, the error limits indicate the systematic errors such as measurement in the concentrations and temperature. The Arrhenius plot of the rate coefficients measured for the title reaction is shown in Figure 3. We observed a very low positive temperature dependence on rate coefficients for this reaction within our experimental uncertainties. The linear least-squares fit of our measured rate coefficients between 288 and

DOI: 10.1021/jp509800g
J. Phys. Chem. A 2015, 119, 559−570

Table 1. Concentrations (Units: molecules cm^{-3}), Rate Coefficient Ratios, and Rate Coefficients (Units: cm^3 molecule^{-1} s^{-1}) of Cl Atoms with *p*-Cymene over the Temperature Range 288−350 K and at 700-800 Torr in N_2/Air

T (K)	reference	bath gas	[*p*-cymene]	[reference]	$[(COCl)_2]$	$(k_{p\text{-cymene}}/k_{ref})^a$	$(k_{p\text{-cymene}}/k_{ref})_{avr}{}^b$	$k \times 10^{10}$ ^{c}	literature (298 K) $k \times 10^{10}$
288	ethylene	N_2	5.2×10^{16}	4.3×10^{15}	1.1×10^{17}	1.33 ± 0.42	1.61 ± 0.52	1.70 ± 1.15	2.10 ± 0.4 (Finlayson-Pitts et al.)[36]
		N_2	5.3×10^{16}	5.3×10^{15}	8.6×10^{16}	1.88 ± 0.15			
		air	4.6×10^{16}	3.1×10^{17}	5.6×10^{17}	1.39 ± 0.09	1.56 ± 0.57	1.65 ± 1.15	
		air	4.6×10^{16}	3.7×10^{17}	6.3×10^{17}	1.67 ± 0.23			
		air	4.6×10^{16}	1.7×10^{17}	6.4×10^{17}	1.62 ± 0.25			
298	1,3-butadiene	N_2	4.6×10^{16}	8.3×10^{15}	2.6×10^{17}	0.74 ± 0.05	0.79 ± 0.17	3.30 ± 0.78	
		N_2	4.6×10^{16}	1.2×10^{16}	2.4×10^{17}	0.73 ± 0.09			
		N_2	4.6×10^{16}	1.0×10^{16}	2.2×10^{17}	0.89 ± 0.10			
		N_2	4.5×10^{16}	5.1×10^{15}	1.4×10^{17}	0.89 ± 0.08			
		N_2	4.6×10^{16}	7.2×10^{15}	2.1×10^{17}	0.69 ± 0.07			
		N_2	4.9×10^{16}	6.6×10^{15}	2.8×10^{17}	0.77 ± 0.05			
	ethylene	N_2	5.1×10^{16}	1.0×10^{16}	2.8×10^{17}	2.14 ± 0.29	1.97 ± 0.53	1.86 ± 1.22	
		N_2	5.2×10^{16}	5.3×10^{15}	2.1×10^{17}	1.82 ± 0.38			
		N_2	5.2×10^{16}	1.8×10^{15}	4.2×10^{17}	1.94 ± 0.21			
		air	4.7×10^{16}	1.8×10^{16}	2.5×10^{17}	1.60 ± 0.14	1.70 ± 0.34	1.61 ± 1.01	
		air	5.2×10^{16}	5.0×10^{16}	2.6×10^{17}	1.86 ± 0.25			
		air	4.6×10^{16}	7.0×10^{15}	4.7×10^{17}	1.64 ± 0.20			
310	ethylene	N_2	5.2×10^{16}	2.6×10^{15}	2.0×10^{17}	2.14 ± 0.20	2.21 ± 0.36	1.85 ± 1.14	
		N_2	5.2×10^{16}	1.7×10^{15}	3.9×10^{17}	2.28 ± 0.30			
325	ethylene	N_2	5.2×10^{16}	2.6×10^{15}	3.9×10^{17}	3.10 ± 0.28	3.04 ± 0.44	2.20 ± 1.35	
		N_2	5.2×10^{16}	1.8×10^{15}	4.0×10^{17}	2.97 ± 0.34			
340	ethylene	N_2	5.2×10^{16}	3.5×10^{15}	4.3×10^{17}	3.70 ± 0.48	3.65 ± 0.64	2.33 ± 1.44	
		N_2	$4. \times 10^{16}$	4.6×10^{15}	4.0×10^{17}	3.59 ± 0.43			
350	ethylene	N_2	5.1×10^{16}	4.3×10^{15}	1.1×10^{17}	3.62 ± 0.26	3.73 ± 0.57	2.19 ± 1.35	
		N_2	5.2×10^{16}	3.5×10^{15}	1.2×10^{17}	3.83 ± 0.52			
		air	4.8×10^{16}	9.2×10^{16}	5.7×10^{17}	3.52 ± 0.62	3.54 ± 1.04	2.08 ± 1.37	
		air	8.7×10^{16}	1.7×10^{17}	1.2×10^{18}	3.55 ± 0.80			

^{a}Indicated errors are two least-squares standard deviations and are obtained from linear least-squares fitting of the data. ^{b}Indicated errors on the average values of the slopes are determined using the error propagation method according to the following equation: $\Delta y/y = [[\Delta a/a]^2 + [\Delta b/b]^2 + ...]^{1/2}$, where $\Delta y/y$ is the relative error on the average slope and $[\Delta a/a]$, $[\Delta b/b]$, ..., are the relative errors on the individual slopes. ^{c}Indicated errors are two least-squares standard deviations and include uncertainties in the rate coefficients of reference compounds by using the error propagation method according to the following equation: $\Delta k_{p\text{-cymene}} = k_{p\text{-cymene}} \times [(\Delta k_{ref}/k_{ref})^2 + [\Delta(k_{p\text{-cymene}}/k_{ref})/(k_{p\text{-cymene}}/k_{ref})]^2]^{1/2}$, where $(\Delta k_{ref}/k_{ref})$ and $\Delta(k_{p\text{-cymene}}/k_{ref})/(k_{p\text{-cymene}}/k_{ref})$ are the relative errors on k_{ref} and $k_{p\text{-cymene}}/k_{ref}$, respectively.

350 K resulted in an Arrhenius expression: $k_{p\text{-cymene}}(288-350) = (9.36 \pm 2.90) \times 10^{-10} \exp[-(488 \pm 98)/T]$ cm^3 molecule^{-1} s^{-1}. It should be noted here that the rate coefficient obtained by using 1,3-butadiene as a reference compound is not used in the determination of the Arrhenius expression. As far as we know, only one experimentally measured rate coefficient is available in the literature at 298 K for the reaction of *p*-cymene with Cl atom. Finlayson-Pitts et al.[36] measured the rate coefficient for the reaction of Cl atom with *p*-cymene and reported it to be $k_{p\text{-cymene}} = (2.10 \pm 0.4) \times 10^{-10}$ cm^3 molecule^{-1} s^{-1} using the relative rate technique, which is in very good agreement with our room temperature value of $k_{p\text{-cymene}} = (1.86 \pm 1.22) \times 10^{-10}$ cm^3 molecule^{-1} s^{-1} using ethylene as a reference compound. However, our reported rate coefficient at 298 K using 1,3-butadiene as a reference compound is 2 times larger ($k_{p\text{-cymene}}(298\ K) = (3.30 \pm 0.78) \times 10^{-10}$ cm^3 molecule^{-1} s^{-1}) than using ethylene as a reference compound, i.e., $k_{p\text{-cymene}} = (1.86 \pm 1.22) \times 10^{-10}$ cm^3 molecule^{-1} s^{-1}. The discrepancies between the two results may be due to the errors associated with the measurements of the reference compound's rate coefficients, for their reactions with Cl atoms. Ragains and Finlayson-Pitts[50] and Coquet and Ariya[51] have determined the rate coefficients of Cl atoms with 1,3-butadiene (*n*-butane as reference compound) and ethylene (*n*-hexane as reference compound), respectively, using the relative rate technique. The errors reported in these rate coefficients in turn depend on the errors associated with the reference reaction's rate coefficients used in their experiments. Naturally, the systematic errors would propagate into our results as well. Therefore, the average rate coefficient for the title reaction at 298 K is estimated by taking the average of both rate coefficients, i.e., $k_{p\text{-cymene}}(298\ K) = (2.58 \pm 1.55) \times 10^{-10}$ cm^3 molecule^{-1} s^{-1}, which is very close to the literature value $(2.10 \pm 0.4) \times 10^{-10}$ cm^3 molecule^{-1} s^{-1} reported by Finlanson-Pitts et al.[36]

3.2. Computational. *3.2.1. Electronic Structures and Energetics.* For the sake of simplicity, optimized structures at the MP2(FULL)/6-31G(d) level of theory are presented in Figure 4. Different conformers may be possible for *p*-cymene. However, the most stable conformer was used in this study. The conformer for *p*-cymene used in this study is similar to the 3D conformer of *p*-cymene in the pubchem database.[55] In Figure 4, it is clear that there are six possible pathways for the addition of a Cl atom to the aromatic ring of *p*-cymene. Additions of a Cl atom at the C_1 and C_4 carbons of the aromatic ring lead to the formation of adduct radicals P1 and P4 via transition states TS1 and TS4, respectively, whereas additions of a Cl atom at the C_2 and C_3 carbons (syn to the two methyl groups) and the C_5 and C_6 carbons (anti to the two

DOI: 10.1021/jp509800g
J. Phys. Chem. A 2015, 119, 559−570

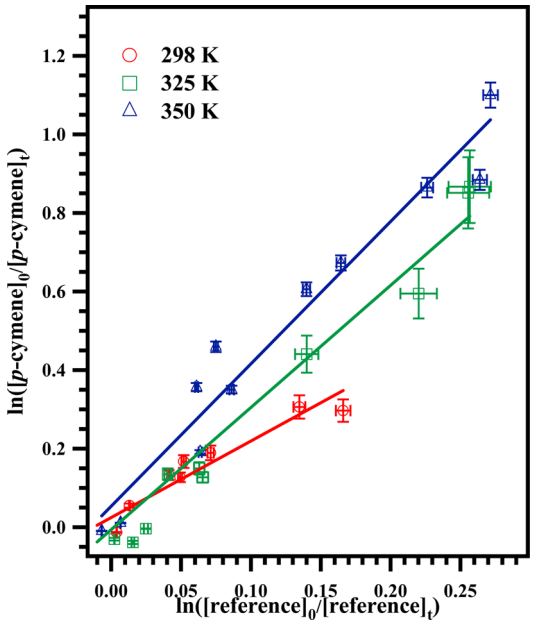

Figure 2. Plot of the relative decrease in the concentration of *p*-cymene due to its reaction with Cl atom at 298, 325, and 350 K in N_2 with ethylene used as a reference compound.

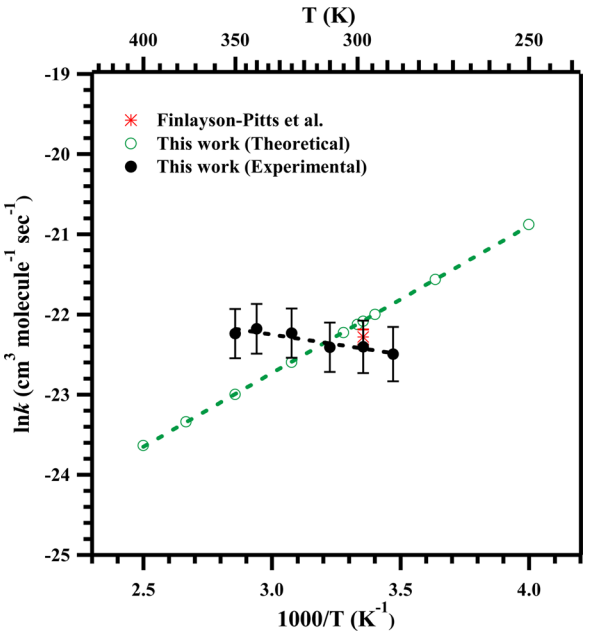

Figure 3. Arrhenius plot of the rate coefficient data obtained for the *p*-cymene + Cl reaction over the temperature range 250−400 K.

methyl groups) of the aromatic ring lead to the formation of adduct radicals P2, P3, P5, and P6 via transition states TS2, TS3, TS5, and TS6, respectively. When the addition takes place between Cl atoms and the double bonds of the aromatic ring in *p*-cymene, they form a stable molecular complex (symmetrically bridged structure; I_{add}) before proceeding to the transition state (asymmetrically bridged structure) and then followed by the corresponding adduct radicals. Six such bridged structures (I_{add1}−I_{add6}) were identified for all six addition channels. Due to these additions at each carbon atom of the aromatic ring, adjacent C—C bond lengths were elongated from ∼1.4 to ∼1.5 Å. For example, due to the addition of a Cl atom at the C_1 carbon, the adjacent C_1—C_2 and C_6—C_1 bond lengths are elongated from 1.400 and 1.398 Å in the aromatic ring to 1.489 Å in the adduct radical P1. This is because of the electron density in the π bond (C═C) shifted to the newly formed σ bond (C—Cl). The lengthening of C—C bond lengths in *p*-cymene at various levels of theory is given in the Supporting Information (Table S.I). In addition to the addition reactions, hydrogen abstraction reactions are also possible in *p*-cymene by Cl atoms from different carbons site leading to the formation of products P7−P13 plus a HCl molecule via transition states TS7−TS13, respectively. TS7 corresponds to the abstraction of a hydrogen atom from the tertiary carbon atom (C_{15}) of the isopropyl group, TS8−TS10 correspond to the abstraction of hydrogen from the methyl group (C_{11}), and TS11−TS13 correspond to the abstraction of hydrogen from the isopropyl group (C_{17}) of *p*-cymene (Figure 4). However, the transition states corresponding to the abstraction of hydrogen from aromatic carbons atoms (C_2, C_3, C_5, and C_6) could not be located. In all abstraction TSs of the *p*-cymene + Cl reaction, the lengths of the breaking C—H bonds are elongated between 19 and 25% when compared to the C—H equilibrium bond length in *p*-cymene, while the lengths of the forming H—Cl bond are elongated between 10 and 15% more than the equilibrium bond length of HCl. The elongation of the breaking bond is larger than that of the forming bond, indicating that the transition states are product-like and the reactions proceed through "late transition states". There is not much difference in the bond lengths between different levels of theory. The elongation of the bond length between the C—H and H—Cl bonds of reactants and TSs at various levels of theory is given in the Supporting Information (Table S.II). The vibrational frequencies and structural parameters of the reactants, intermediates (I_{adds}), transition states (TSs), and products in the *p*-cymene + Cl reaction are given in the Supporting Information (Tables S.III and S.IV).

The relative energies ($\Delta E_0^{\ddagger}$ in kcal mol^{-1}) including the zero point energy (ZPE) obtained for all TSs using different theoretical levels are summarized in Table 2. Single point energy calculations using QCISD(T)/6-31G(d,p) with the optimized geometries at the MP2/6-31G(d,p) level of theory give less stable relative energies than the single point energy calculations using QCISD(T)/6-31G(d), QCISD(T)/6-31+G-(d,p), and QCISD(T)/6-311++G(d,p) with the optimized geometries at the MP2(FULL)/6-31G(d) level of theory. As the Pople basis sets extended in single point energy calculations using QCISD(T) with the optimized geometries at the MP2(FULL)/6-31G(d) level of theory, the stability of all transition states are found to be increasing. Single point energy calculations using CCSD(T) with the optimized geometries at MP2(FULL)/6-31G(d) give less stable relative energies than the single point energy calculations using QCISD(T) with the optimized geometries at the same level of theory. On the other hand, single point energy calculations using CCSD(T)/6-31+G(d,p) with the optimized geometries at MP2(FULL)/6-31G(d) give slightly less stable relative energies than with the optimized geometries at the MP2(FULL)/6-31+G(d,p) level of theory. It should be noted that the relative energies for all abstraction TSs (TS7−TS13) are much higher (Table 2) than the addition TSs (TS1−TS6) at all levels, which suggests that the contributions of abstraction reactions to the total reactions are insignificant. A schematic potential energy (PES) surface of the *p*-cymene + Cl reaction with ZPE corrections obtained at the QCISD(T)/6-31+G(d,p)//MP2(FULL)/6-31G(d) level

DOI: 10.1021/jp509800g
J. Phys. Chem. A 2015, 119, 559−570

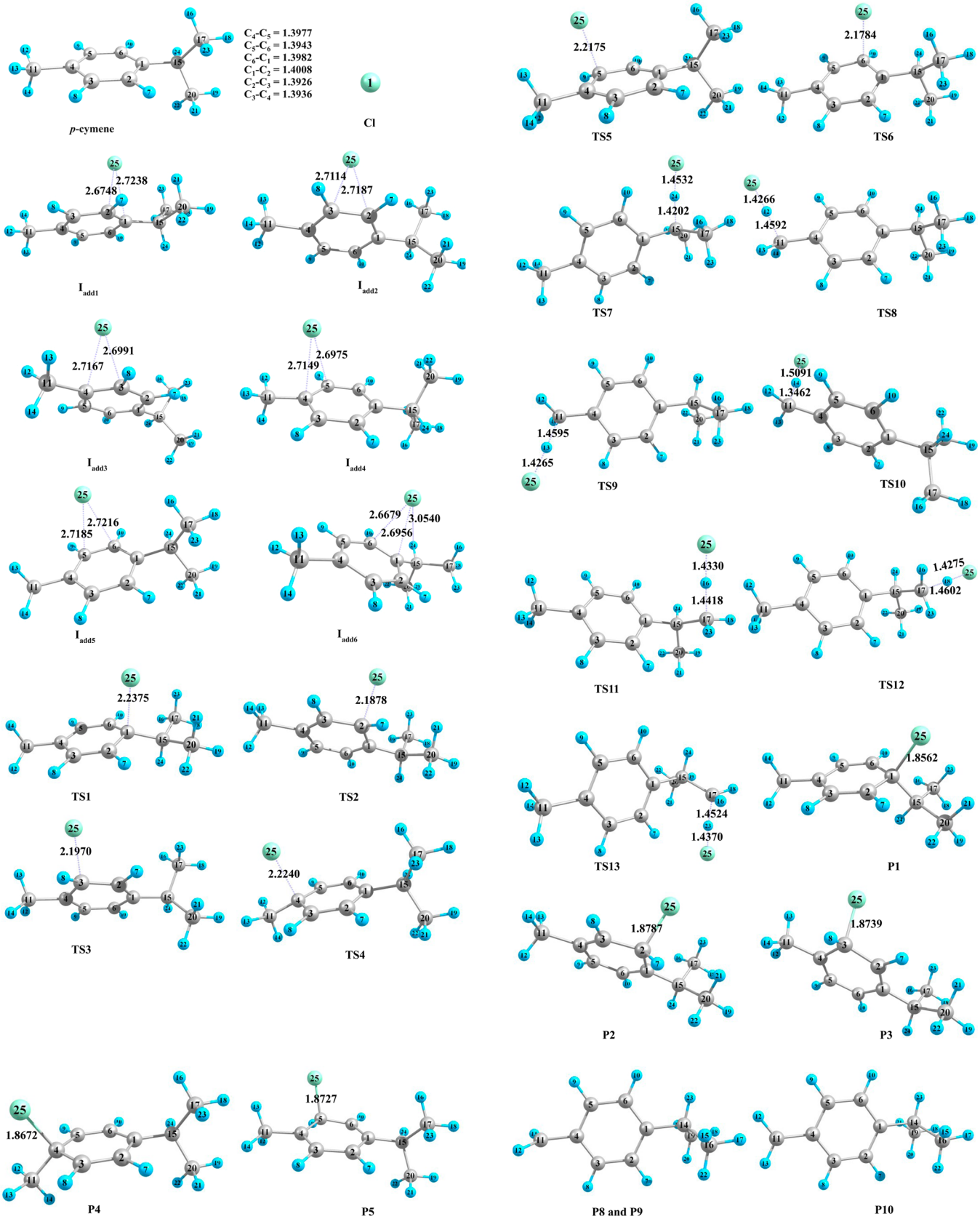

Figure 4. continued

DOI: 10.1021/jp509800g
J. Phys. Chem. A 2015, 119, 559−570

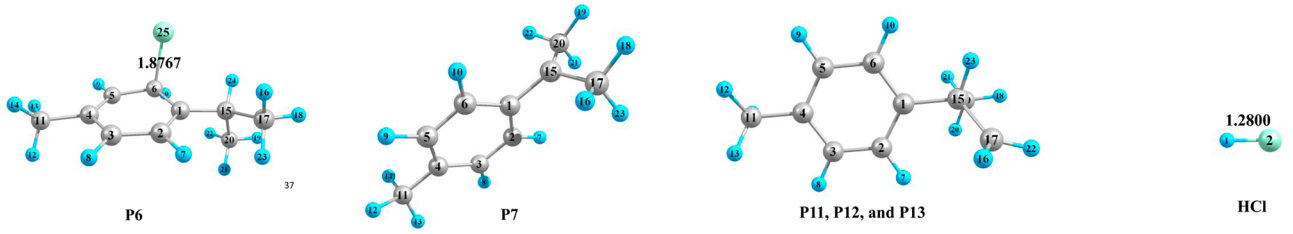

Figure 4. Geometries of the reactants, intermediates (I_{adds}), transition states (TSs), and products optimized at the MP2(FULL)/6-31G(d) level of theory. Sky blue represents hydrogen, black represents carbon, and light green represents chlorine atoms in the structures. The bond lengths (Å) given on the structures are obtained at the MP2(FULL)/6-31G(d) level of theory.

Table 2. Relative Energies ($\Delta E_0^{\ddagger}$, kcal mol^{-1}) Obtained for All TSs in the *p*-Cymene + Cl Reaction at Different Levels of Theory Using Various Basis Sets

TSs	QCISD(T)/ 6-31G(d,p)// MP2/ 6-31G(d,p)	QCISD(T)/ 6-31G(d)// MP2(FULL)/ 6-31G(d)	QCISD(T)/ 6-31+G(d,p)// MP2(FULL)/ 6-31G(d)	QCISD(T)/6-311++G(d,p)// MP2(FULL)/6-31G(d)	CCSD(T)/ 6-31G(d)// MP2(FULL)/ 6-31G(d)	CCSD(T)/ 6-31+G(d,p)// MP2(FULL)/ 6-31G(d)	CCSD(T)/ 6-31+G(d,p)// MP2(FULL)/ 6-31+G(d,p)
TS1	1.30	1.27	−1.40	−4.26	1.59	−1.02	−1.18
TS2	−0.72	−0.85	−2.57	−5.53	−0.56	−2.22	−2.39
TS3	−1.53	−1.92	−3.46	−5.78	−1.63	−3.12	−3.17
TS4	−1.08	−1.16	−3.50	−5.82	−0.86	−3.13	−3.25
TS5	−1.98	−2.16	−3.70	−5.96	−1.88	−3.36	−3.49
TS6	−1.49	−1.63	−3.60	−6.09	1.34	−3.24	−3.36
TS7	2.09	4.46	−0.63	−3.29	4.58	−0.49	−0.40
TS8	9.90	12.91	8.40	5.26	13.02	8.53	8.69
TS9	9.89	12.90	8.38	5.24	13.00	8.52	8.68
TS10	8.37	10.48	6.23	3.69	10.62	6.42	6.77
TS11	10.09	12.92	7.42	4.30	12.99	7.52	7.53
TS12	8.86	11.70	7.05	3.97	11.79	7.16	7.17
TS13	9.49	12.30	7.50	4.09	12.38	7.59	7.56

of theory is plotted in Figure 5. It is clear from this figure that all the abstraction reactions are endothermic in nature except the reaction path going through a transition state, TS10 (one of the methyl-H abstraction), in which the energies of the products are slightly below those of the reactants (−0.26 kcal mol^{-1}). It is obvious from the PES that the energies of some of the products in abstraction reactions are above those of the transition states, which shows that the abstractions reactions are not favorable reaction pathways. On the other hand, the energies of the products obtained in addition reactions are below those of the reactants and therefore they are favorable reaction pathways. The entropies of activation ($\Delta S^{\ddagger}$ in cal mol^{-1} K^{-1}) for both addition and abstraction channels are obtained at various levels of theory and are given in Table 3. $\Delta S^{\ddagger}$ values for the addition channels are found to be more negative than those for the abstraction channels, which shows that the addition TSs are less disordered than the abstraction TSs.

3.2.2. Rate Coefficients. As discussed above, the abstraction reactions are not favorable and their contributions to the total reactions are insignificant; therefore, rate coefficients were calculated for only addition pathways. The dual level direct dynamic approach was used to study the initial step in the reactions of *p*-cymene with Cl atoms. The rate coefficients are calculated by variational transition state theory (VTST) with the interpolated single-point energy[56] (ISPE) methods, developed by Truhlar et al. The relative energies calculated for all addition TSs (TS1−TS6) at the QCISD(T)/6-311++G(d,p)//MP2(FULL)/6-31G(d) level of theory were used in these VTST/ISPE calculations. Energies obtained at other levels are observed to be lower estimated (this observation is made on the basis of the rate coefficients measured in the current investigations and the available experimentally determined rate coefficients). The details of the computational methodologies were described elsewhere in our recently reported article.[39] The CVT and CVT/SCT rate coefficients (in cm^3 molecule^{-1} s^{-1}) for the *p*-cymene + Cl reaction in the temperature range 250−400 K along with the present experimental and literature values at room temperature are given in Table 4. The rate coefficients (in cm^3 molecule^{-1} s^{-1}) for the *p*-cymene + Cl reaction (Table 4) are obtained from the sum of the individual rate coefficients ($k = k_{TS1} + k_{TS2} + k_{TS3} + k_{TS4} + k_{TS5} + k_{TS6}$). The CVT/SCT rate coefficients of the various addition channels (k_{TS1}−k_{TS6}) for the *p*-cymene + Cl reaction over the temperature range 250−400 K at the QCISD(T)/6-31+G(d,p)//MP2(FULL)/6-31G(d) level of theory are given in Table 5. The calculated room temperature rate coefficient for the *p*-cymene + Cl is 2.56 × 10^{-10} cm^3 molecule^{-1} s^{-1}, which is in excellent agreement with our experimentally measured rate coefficient (2.58 ± 1.55) × 10^{-10} cm^3 molecule^{-1} s^{-1} at room temperature using the relative rate technique and ∼20% higher than the reported rate coefficient (measured experimentally) by Finlayson-Pitts et al.[36] using the relative rate technique, with nonane as a reference compound, i.e., (2.10 ± 0.4) × 10^{-10} cm^3 molecule^{-1} s^{-1}. All the experimental findings were based on the relative rate technique to determine the rate coefficient, which depends on the accuracy of the reported rate coefficient of the reference reaction. At room temperature, the total rate coefficient for the Cl atom reaction with *p*-cymene is found to be 2 times larger

DOI: 10.1021/jp509800g
J. Phys. Chem. A 2015, 119, 559−570

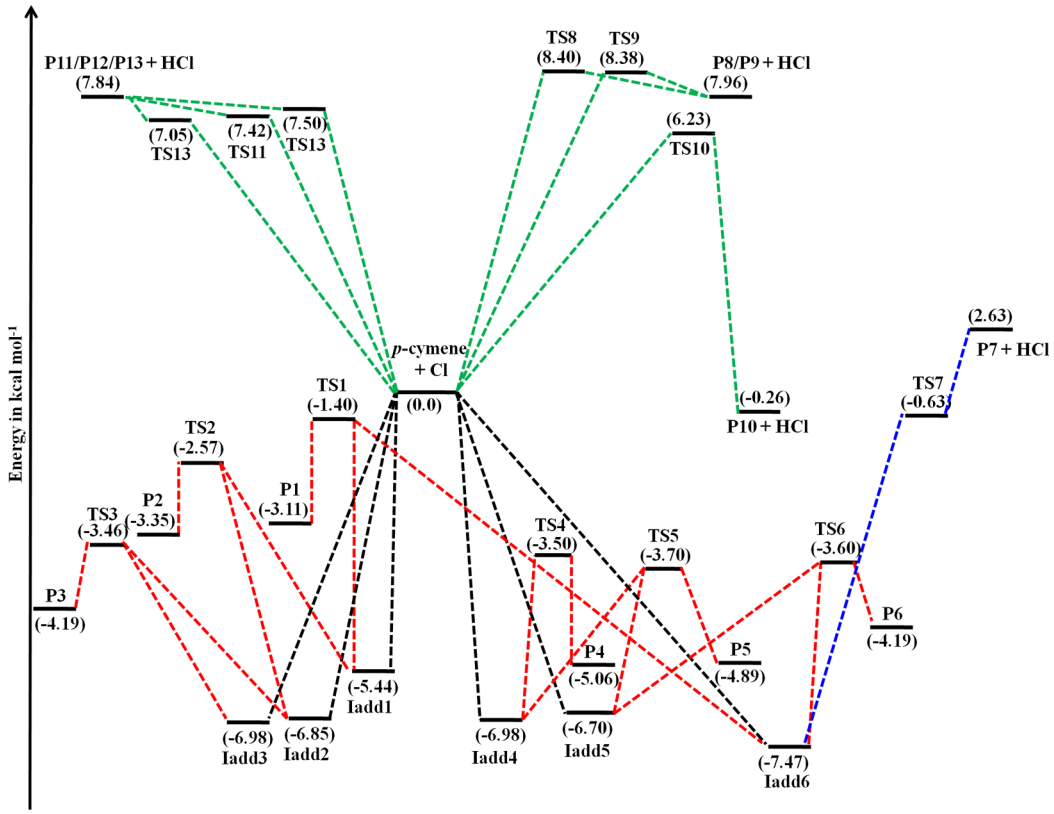

Figure 5. Energy level diagram for the *p*-cymene + Cl reaction through all the transition states obtained at the QCISD(T)/6-31+G(d,p)//MP2(FULL)/6-31G(d) level of theory. The energies are given in the units of kcal mol^{-1}. Red dotted lines: addition pathways. Blue dotted lines: tertiary hydrogen abstraction pathways. Green dotted lines: primary hydrogen abstraction pathways.

Table 3. Entropy of Activation ($\Delta S^{\ddagger}$, cal mol^{-1} K^{-1}) Obtained for the *p*-Cymene + Cl Reaction at Different Levels of Theory

	MP2/6-31G(d)	MP2/6-31G(d,p)	MP2/6-31+G(d,p)	MP2(FULL)/6-31G(d)	MP2(FULL)/6-31+G(d,p)
TS1	−31.19	−30.86	−31.38	−31.09	−31.23
TS2	−31.86	−31.50	−31.88	−31.87	−31.90
TS3	−29.44	−29.00	−28.42	−29.16	−28.12
TS4	−31.83	−31.67	−32.04	−31.75	−31.98
TS5	−30.54	−30.28	−30.45	−30.49	−30.47
TS6	−29.89	−29.73	−30.14	−29.86	−30.11
TS7	−25.44	−25.60	−26.99	−25.50	−26.97
TS8	−27.01	−26.99	−26.90	−27.03	−26.96
TS9	−27.03	−27.02	−26.89	−27.06	−26.94
TS10	−28.14	−27.96	−27.87	−28.06	−27.94
TS11	−23.98	−24.10	−25.22	−23.92	−25.24
TS12	−24.49	−24.59	−24.61	−24.47	−24.63
TS13	−25.55	−25.43	−25.48	−25.47	−25.91

than the ones measured for *o*-, *m*-, and *p*-xylene and 3 times larger than the one measured for toluene. Wallington et al.,[57] Shi and Bernhard,[58] and Anderson et al.[59] reported the rate coefficients for the Cl atom reaction with *o*-, *m*-, and *p*-xylene which fall in the range $(1.2-1.5) \times 10^{-10}$ cm^3 $molecule^{-1}$ s^{-1}. The reported values for the Cl atom reaction with toluene at room temperature fall in between 5.6 and 6.1×10^{-11} cm^3 $molecule^{-1}$ s^{-1}.[57,58,60−64] The experimental results on the reaction products and isotope effects indicate that the reactions of Cl atom with alkyl aromatics like toluene, xylene, alkyl naphthalenes, etc., proceed via an abstraction reaction,[65] whereas we have calculated the rate coefficients of the *p*-cymene + Cl reaction only for addition channels. However, we cannot rule out the contribution or even the dominance of abstraction channels especially through the low lying transition states. Therefore, it is difficult to conclude from our calculations that abstraction channels cannot contribute to this reaction. This question still needs to be understood probably via carrying out further experiments.

The Arrhenius plot of the rate coefficient data obtained using CVT/SCT calculations in the temperature range 250−400 K is depicted in Figure 3. The rate coefficients exhibit a negative temperature dependence, and the data were fit by the linear least-squares formula. The obtained Arrhenius expression is $k(T) = 5.41 \times 10^{-13} \exp[1837/T]$ cm^3 $molecule^{-1}$ s^{-1}. These calculated results are in contrast to the results of our experimentally measured temperature dependent rate coefficients in which a very low positive temperature dependence

DOI: 10.1021/jp509800g
J. Phys. Chem. A 2015, 119, 559−570

Table 4. Rate Coefficients (cm^3 $molecule^{-1}$ s^{-1}) for the *p*-Cymene + Cl Reaction over the Temperature Range 250−400 K at the QCISD(T)/6-311++G(d,p)//MP2(FULL)/6-31G(d) Level of Theory

T (K)	CVT	CVT/SCT	present experimental and literature values
250	1.08×10^{-9}	8.55×10^{-10}	
275	5.34×10^{-10}	4.31×10^{-10}	
298	3.11×10^{-10}	2.56×10^{-10}	
300	2.98×10^{-10}	2.46×10^{-10}	$(2.58 \pm 1.55) \times 10^{-10}$ (present experiment), $(2.10 \pm 0.4) \times 10^{-10}$ (Finlayson-Pitts et al.)[36]
325	1.83×10^{-10}	1.53×10^{-10}	
350	1.21×10^{-10}	1.03×10^{-10}	
375	8.49×10^{-11}	7.29×10^{-11}	
400	6.27×10^{-11}	5.43×10^{-11}	

on rate coefficients for this reaction was observed. This slope is insignificant if the errors are considered, and the rate coefficients are independent of temperature, as observed in most of the Cl atom reactions (Table 1). The discrepancy between the theoretically calculated rate coefficients and experimentally measured rate coefficients is unclear. One possible source of error in the measurement of rate coefficients is the uncertainty associated with the available reference reaction's rate coefficient value. On the other hand, in theoretical calculations as discussed before, there are large uncertainties associated with the energies for the low lying addition TSs below the energy of the reactants at various levels of theory. Also, the theoretically calculated pre-exponential factor depends mainly on how best the partition functions of both the reactants and transition state are estimated, which in turn depends on the vibrational frequencies obtained using the chosen theory for these calculations. Therefore, absolute methods of experimentation like laser-induced fluorescence (LIF) should be employed to get a clear picture on the rate coefficients.

3.2.3. Branching Ratios. The branching ratios of individual addition channels over the whole temperature range 250−400 K are given in Figure 6. It is clear from this figure that the additions of a Cl atom at the C_6 and C_3 carbons are the major contributors to the total rate coefficients, whereas addition at the C_4, C_5, and C_2 carbons are moderate contributors and addition at the C_1 carbon is a negligible contributor to the total rate coefficients in the studied temperature range. For example, the k_{TS6}/k (C_6), k_{TS3}/k (C_3), k_{TS4}/k (C_4), k_{TS5}/k (C_5), and k_{TS2}/k (C_2) ratios are 0.45, 0.22, 0.16, 0.10, and 0.07 at 250 K and 0.41, 0.23, 0.15, 0.09, and 0.10 at 400 K, respectively. These values suggest that the contribution of Cl atom additions at the C_3, C_4, and C_5 carbons to the total rate coefficients is constant over the studied temperature range, while the contribution of

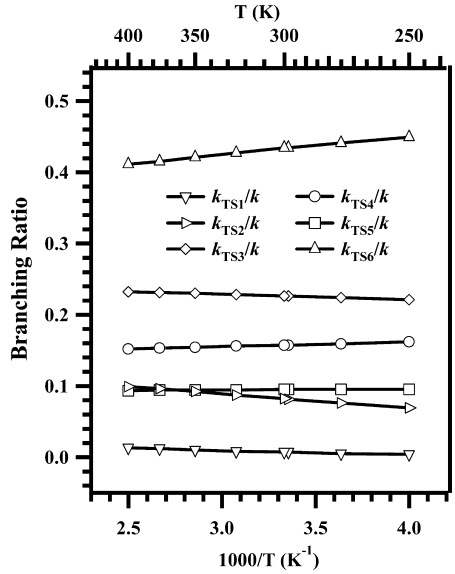

Figure 6. Calculated branching ratios of k_{TS1}, k_{TS2}, k_{TS3}, k_{TS4}, k_{TS5}, and k_{TS6} to the total rate coefficient for the *p*-cymene + Cl reaction over the temperature range 250−400 K.

Cl atom addition at the C_6 carbon slowly decreases with an increase in temperature and the contribution of Cl atom addition at the C_2 carbon slowly increases with an increase in temperature. These values also suggest that the anti addition (C_6) is more favorable than the syn addition (C_2), which is obvious.

4. ATMOSPHERIC IMPLICATIONS

Atmospheric degradation of *p*-cymene mainly occurs via its reactions with tropospheric oxidants like OH radicals, NO_3 radicals, and Cl atoms. The atmospheric lifetimes (τ) of *p*-cymene due to its reactions with the above oxidants were calculated according to the equation $\tau = 1/k[\text{oxidant}]$, where [oxidant] is the average concentration of the oxidant and k is the rate coefficient of *p*-cymene with the oxidant at 298 K. The global average concentrations used in the calculations are 1×10^6 radicals cm^{-3}, 1×10^3 atoms cm^{-3}, and 2.5×10^8 radicals cm^{-3} for OH,[66] Cl,[19,20] and NO_3,[67] respectively. By using the rate coefficients of *p*-cymene with Cl atoms (present experimental and theoretical investigations), OH radicals (8.2×10^{-12} and 1.51×10^{-11} $cm^3 molecule^{-1}$ s^{-1}),[34,35] and NO_3 radicals (9.9×10^{-16} $cm^3 molecule^{-1}$ s^{-1}),[33] the atmospheric lifetimes of *p*-cymene were calculated and are given in Table 6. It is clear from Table 6 that the reaction with OH radical plays a major role in the degradation process of *p*-cymene during the

Table 5. CVT/SCT Rate Coefficients (cm^3 $molecule^{-1}$ s^{-1}) of the Various Addition Channels for the *p*-Cymene + Cl Reaction over the Temperature Range 250−400 K at the QCISD(T)/6-311++G(d,p)//MP2(FULL)/6-31G(d) Level of Theory

T (K)	k_{TS1}	k_{TS2}	k_{TS3}	k_{TS4}	k_{TS5}	k_{TS6}
250	3.49×10^{-12}	5.91×10^{-11}	1.89×10^{-10}	1.38×10^{-10}	8.12×10^{-11}	3.84×10^{-10}
275	2.35×10^{-12}	3.26×10^{-11}	9.65×10^{-11}	6.87×10^{-11}	4.08×10^{-11}	1.90×10^{-10}
298	1.74×10^{-12}	2.08×10^{-11}	5.78×10^{-11}	4.02×10^{-11}	2.42×10^{-11}	1.11×10^{-10}
300	1.70×10^{-12}	2.00×10^{-11}	5.56×10^{-11}	3.85×10^{-11}	2.32×10^{-11}	1.06×10^{-10}
325	1.30×10^{-12}	1.33×10^{-11}	3.49×10^{-11}	2.38×10^{-11}	1.45×10^{-11}	6.53×10^{-11}
350	1.04×10^{-12}	9.40×10^{-12}	2.36×10^{-11}	1.58×10^{-11}	9.65×10^{-12}	4.32×10^{-11}
375	8.56×10^{-13}	6.98×10^{-12}	1.68×10^{-11}	1.11×10^{-11}	6.83×10^{-12}	3.02×10^{-11}
400	7.25×10^{-13}	5.39×10^{-12}	1.26×10^{-11}	8.23×10^{-12}	5.07×10^{-12}	2.23×10^{-11}

DOI: 10.1021/jp509800g
J. Phys. Chem. A 2015, 119, 559−570

Table 6. Calculated Atmospheric Lifetimes of *p*-Cymene due to Its Reaction with Various Tropospheric Oxidants

τ_{Cl}[a] (days)		τ_{Cl}[b] (hours)		τ_{OH}[c] (hours)		τ_{NO_3}[d] (days)
present experiment	CVT/SCT	present experiment	CVT/SCT	Dash and Rajakumar[35]	Alarcon et al.[34]	Corchnoy and Atkinson[33]
45	45	8	8	34	18	47

[a]Cl atom average concentration, [Cl] = 10^3 atoms cm^{-3} (Singh et al.).[19] [b]Coastal and marine boundary layer, [Cl] = 1.3×10^5 atoms cm^{-3} (Spicer et al.).[21] [c]OH radical average concentration, [OH] = 1.0×10^6 radicals cm^{-3} (Prinn et al.).[66] [d]NO_3 radical average concentration, [NO_3] = 2.5×10^8 radicals cm^{-3} (Atkinson).[67]

daytime and reaction with NO_3 will be competitive during the nighttime. The reaction of *p*-cymene with Cl atoms is not very important in ambient conditions because the global average concentration of the chlorine atom is as low as 10^3 atoms cm^{-3} [19,20] compared to other tropospheric oxidants. However, the reaction of *p*-cymene with Cl atoms can compete with OH radicals in coastal and urban industrial areas, where the peak concentration of Cl atoms will be 1.3×10^5 atoms cm^{-3}.[21] The lifetime calculated with this concentration is 8.3 h and the OH-driven atmospheric lifetimes are 18−34 h, which are comparable.

5. CONCLUSIONS

The kinetics of the reaction of *p*-cymene with Cl atoms was investigated using the relative rate technique and *ab initio* methods. This work represents the first kinetic study of the reaction of Cl atoms with *p*-cymene as a function of temperature. In experiment, a very low positive temperature dependence on the rate coefficients for the *p*-cymene + Cl reaction was observed in contrast to the negative temperature dependence observed with theoretical calculations. The PES of the title reaction shows that the abstraction channels are unfavorable reaction pathways. The reaction is completely governed by addition of Cl at various double bonded sites. Although the addition channels seem to be dominating, we cannot rule out the significance contribution or the domination of the abstraction channels especially when they are low lying. This question still needs to be understood probably via carrying out further experiments. The calculated atmospheric lifetime data suggest that the removal of *p*-cymene mainly occurs in the atmosphere via its reaction with OH radicals. However, in the coastal and marine boundary layer where Cl atom concentrations are high, both OH radical and Cl atom reactions will compete.

■ ASSOCIATED CONTENT

Supporting Information

Tables S.I to S.IV (bond distances, vibrational frequencies, and Cartesian coordinates). This material is available free of charge via the Internet at http://pubs.acs.org.

■ AUTHOR INFORMATION

Corresponding Author

*Phone: +91-44-22574231. E-mail: rajakumar@iitm.ac.in.

Notes

The authors declare no competing financial interest.

■ ACKNOWLEDGMENTS

The authors thank Professor Donald G. Truhlar and his group for providing the POLYRATE 2008 and GAUSSRATE 2009A programs. Also, the authors thank the High Performance Computing Centre and Mr. V. Ravichandran for providing computer resources. B.R. thanks the BRNS, Government of India (Sanction No. 2012/37C/22/BRNS), for the research funding.

■ REFERENCES

(1) Guenther, A.; Hewitt, C. N.; Erickson, D.; Fall, R.; Geron, C.; Graedel, T.; Harley, P.; Klinger, L.; Lerdau, M.; McKay, W. A.; et al. A Global Model of Natural Volatile Organic Compound Emissions. *J. Geophys. Res.* **1995**, *100*, 8873−8892.

(2) Guenther, A.; Geron, C.; Pierce, T.; Lamb, B.; Harley, P.; Fall, R. Natural Emissions of Non-Methane Volatile Organic Compounds, Carbon monoxide, and Oxides of Nitrogen from North America. *Atmos. Environ.* **2000**, *34*, 2205−2230.

(3) Sawyer, R. F.; Harley, R. A.; Cadle, S. H.; Norbeck, J. M.; Slott, R.; Bravo, H. A. Mobile Sources Critical Review: 1998 NARSTO assessment. *Atmos. Environ.* **2000**, *34*, 2161−2181.

(4) Placet, M.; Mann, C. O.; Gilbert, R. O.; Niefer, M. J. Emissions of Ozone Precursors from Stationary Sources: A Critical Review. *Atmos. Environ.* **2000**, *34*, 2183−2204.

(5) Rasmussen, R. A. What do the Hydrocarbons from Trees Contribute to Air Pollution. *J. Air Pollut. Control Assoc.* **1972**, *22*, 537−543.

(6) Zimmerman, P. R.; Chatfield, R. B.; Fishmann, J.; Crutzen, P. J.; Hanst, P. L. Estimates on the Production of CO and H_2 from the Oxidation of Hydrocarbon Emissions from Vegetation. *Geophys. Res. Lett.* **1978**, *5*, 679−682.

(7) Lamb, B.; Guenther, A.; Gay, D.; Westberg, H. A National Inventory of Biogenic Hydrocarbon Emissions. *Atmos. Environ.* **1987**, *21*, 1695−1705.

(8) Fehsenfeld, F. C.; Calvert, J.; Fall, R.; Goldan, P.; Guenther, A. B.; Hewitt, C. N.; Lamb, B.; Liu, S.; Trainer, M.; Westberg, H.; Zimmerman, P. Emissions of Volatile Organic Compounds from Vegetation and Implications for Atmospheric Chemistry. *Global Biogeochem. Cycles* **1992**, *6*, 389−430.

(9) Went, F. W. Blue Hazes in the Atmosphere. *Nature* **1960**, *197*, 641−643.

(10) Pandis, S. N.; Paulson, S. E.; Seinfeld, J. H.; Flagan, R. C. Aerosol Formation in the Photooxidation of Isoprene and β-Pinene. *Atmos. Environ.* **1991**, *25*, 997−1008.

(11) Hoffmann, T.; Odum, J. R.; Bowman, F.; Collins, D.; Klockow, D.; Flagan, R. C.; Seinfeld, J. H. Formation of Organic Aerosols from the Oxidation of Biogenic Hydrocarbons. *J. Atmos. Chem.* **1997**, *26*, 189−222.

(12) Jacob, D.; Wofsy, S. Photochemistry of Biogenic Emissions Over the Amazon Forest. *J. Geophys. Res.* **1998**, *93*, 1477−1486.

(13) Rizzo, L. V.; Artaxo, P.; Karl, T.; Guenther, A. B.; Greenberg, J. Aerosol Properties, In-canopy Gradients, Turbulent Fluxes and VOC Concentrations at a Pristine Forest Site in Amazonia. *Atmos. Environ.* **2010**, *44*, 503−511.

(14) Charlson, R. J.; Schwartz, S. E.; Hales, J. M.; Cess, R. D.; Coakley, J. A., Jr.; Hansen, J. E.; Hofmann, J. H. Climate Forcing by Anthropogenic Aerosols. *Science* **1992**, *255*, 423−430.

(15) Novakov, T.; Penner, J. E. Large Contribution of Organic Aerosols to Cloud-Condensation Nuclei Concentrations. *Nature* **1993**, *365*, 823−826.

(16) Cruz, C. N.; Pandis, S. N. A Study of the Ability of Pure Secondary Organic Aerosol to act as Cloud Condensation Nuclei. *Atmos. Environ.* **1997**, *31*, 2205−2214.

DOI: 10.1021/jp509800g
J. Phys. Chem. A 2015, 119, 559−570

(17) Zhang, R.; Suh, I.; Zhao, J.; Zhang, D.; Fortner, E. C.; Tie, X.; Molina, L. T.; Molina, M. J. Atmospheric New Particle Formation Enhanced by Organic Acids. *Science* **2004**, *304*, 1487−1490.
(18) Thornton, J. A.; Kercher, J. P.; Riedel, T. P.; Wagner, N. L.; Cozic, J.; Holloway, J. S.; Dube, W. P.; Wolfe, G. M.; Quinn, P. K.; Middlebrook, A. M.; et al. A Large Atomic Chlorine Source Inferred from Mid-Continental Reactive Nitrogen Chemistry. *Nature* **2010**, *464*, 271−274.
(19) Singh, H. B.; Thakur, A. N.; Chen, Y. E.; Kanakidou, M. Tetrachloroethylene as an Indicator of Low Cl Atom in the Troposphere. *Geophys. Res. Lett.* **1996**, *23*, 1529−1532.
(20) Wingenter, O. W.; Blake, D. R.; Blake, N. J.; Sive, B. C.; Rowland, F. S.; Atlas, E.; Flocke, F. J. Tropospheric Hydroxyl and Atomic Chlorine Concentrations, and Mixing Timescales Determined from Hydrocarbon and Halocarbon Measurements Made Over the Southern Ocean. *J. Geophys. Res.* **1999**, *104*, 21819−21828.
(21) Spicer, C. W.; Chapman, E. G.; Finlayson-Pitts, B. J.; Plastridge, R. A.; Hubbe, J. M.; Fast, J. D.; Berkowitz, C. M. Unexpectedly High Concentrations of Molecular Chlorine in Coastal Air. *Nature* **1998**, *394*, 353−356.
(22) George, C.; Behnke, W.; Zetzsch, C. Radicals in the Atmosphere: A Changing World! *ChemPhysChem* **2010**, *11*, 3059−3062.
(23) Ravishankara, A. R. Are Chlorine Atoms Significant Tropospheric Free Radicals? *Proc. Natl. Acad. Sci. U.S.A.* **2009**, *106*, 13639−13640.
(24) Glasow, R. V. Atmospheric Chemistry: Wider Role for Airborne Chlorine. *Nature* **2010**, *464*, 168−169.
(25) Osthoff, H. D.; Roberts, J. M.; Ravishankara, A. R.; Williams, E. J.; Lerner, B. M.; Sommariva, R.; Bates, T. S.; Coffman, D.; Quinn, P. K.; Dibb.; et al. High Levels of Nitryl Chloride in the Polluted Subtropical Marine Boundary Layer. *Nat. Geosci.* **2008**, *1*, 324−328.
(26) Bonsang, B.; Polle, C.; Lambert, G. Evidence for Marine Production of Isoprene. *Geophys. Res. Lett.* **1992**, *19*, 1129−1132.
(27) Moore, R. M.; Oram, D. E.; Penkett, S. A. Production of Isoprene by Marine Phytoplankton Cultures. *Geophys. Res. Lett.* **1994**, *21*, 2507−2510.
(28) Milne, P. J.; Reimer, D. D.; Zika, R. G.; Brand, L. E. Measurement of Vertical Distribution of Isoprene in Surface Seawater, its Chemical Fate, and its Emission from Several Phytoplankton Monocultures. *Mar. Chem.* **1995**, *48*, 237−244.
(29) McKay, W. A.; Turner, M. F.; Jones, B. M. R.; Halliwell, C. M. Emissions of Hydrocarbons from Marine Phytoplankton—Some Results from Controlled Laboratory Experiments. *Atmos. Environ.* **1996**, *30*, 2583−2593.
(30) Ratte, M.; Bujok, O.; Spitzy, A.; Rudolph, J. Photochemical Alkene Formation in Seawater from Dissolved Organic Carbon: Results from Laboratory Experiments. *J. Geophys. Res.* **1998**, *103*, 5707−5717.
(31) Maleš, Ž.; Plazibat, M.; Bucar, F. Essential Oil of Portenschlagiella Ramosissima from Croatia, A Rich Source of Myristicin. *Croat. Chem. Acta* **2009**, *82*, 725−728.
(32) Aschmann, S. M.; Arey, J.; Atkinson, R. Formation of *p*-Cymene from OH + γ-Terpinene: H-Atom Abstraction from the Cyclohexadiene Ring Structure. *Atmos. Environ.* **2011**, *45*, 4408−4411.
(33) Corchnoy, S. B.; Atkinson, R. Chlorinated Dibenzofurans and Dioxins in Atmospheric Samples from Cities in New York. *Environ. Sci. Technol.* **1990**, *24*, 1502−1506.
(34) Alarcon, P.; Strekowski, R.; Zetzsch, C. Reversible Addition of the OH radical to p-Cymene in the Gas Phase: Kinetic Analysis Assuming formation of A Single Adduct. Part 1. *Phys. Chem. Chem. Phys.* **2013**, *15*, 20105−20114.
(35) Dash, M. R.; Rajakumar, B. Theoretical Investigations on the Kinetics of p-Cymene + OH Reaction. *Chem. Phys. Lett.* **2014**, *597*, 75−85.
(36) Finlayson-Pitts, B.; J. Keoshian, C. J.; Buehler, B.; Ezell, A. A. Kinetics of Reaction of Chlorine Atoms with Some Biogenic Organics. *Int. J. Chem. Kinet.* **1999**, *31*, 491−499.
(37) Dash, M. R.; Rajakumar, B. Experimental and Theoretical Rate Coefficients for the Gas Phase Reaction of β-Pinene with OH Radical. *Atmos. Environ.* **2013**, *79*, 161−171.
(38) Dash, M. R.; Balaganesh, M.; Rajakumar, B. Rate Coefficients for the Gas-Phase Reaction of OH Radical with α-Pinene: An Experimental and Computational Study. *Mol. Phys.* **2014**, *112*, 1495−1511.
(39) Balaganesh, M.; Dash, M. R.; Rajakumar, B. Experimental and Computational Investigation on the Gas Phase Reaction of Ethyl Formate with Cl Atoms. *J. Phys. Chem. A* **2014**, *118*, 5272−5278.
(40) Dash, M. R.; Rajakumar, B. Reaction Kinetics of Cl Atoms with Limonene: An Experimental and Theoretical Study. *Atmos. Environ.* **2014**, *99*, 183−195.
(41) Frisch, M. J.; Trucks, G. W.; Schlegel, H. B.; Scuseria, G. E.; Robb, M. A.; Cheeseman, J. R.; Scalmani, G.; Barone, V.; Mennucci, B.; Petersson, G. A.; et al. *Gaussian 09*, revision B.01; Gaussian, Inc.: Wallingford, CT, 2010.
(42) Gonzalez-Lafont, A.; Truong, T. N.; Truhlar, D. G. Interpolated Variational Transitionstate Theory: Practical Methods for Estimating Variational Transitionstate Properties and Tunneling Contributions to Chemical Reaction Rates from Electronic Structure Calculations. *J. Chem. Phys.* **1991**, *95*, 8875−8894.
(43) Garrett, B. C.; Truhlar, D. G. Generalized Transition State Theory. Classical Mechanical Theory and Applications to Collinear Reactions of Hydrogen Molecules. *J. Phys. Chem.* **1979**, *83*, 1052−1079.
(44) Garrett, B. C.; Truhlar, D. G.; Grev, R. S.; Magnuson, A. W. Improved Treatment Of Threshold Contributions In Variational Transition-State Theory. *J. Phys. Chem.* **1980**, *84*, 1730−1748.
(45) Lu, D. H.; Truong, T. N.; Melissas, V. S.; Lynch, G. C.; Liu, Y. P.; Garrett, B. C.; Steckler, R.; Isaacson, A. D.; Rai, S. N.; Hancock, G. C. *POLYRATE 4*: A New Version Of A Computer Program For The Calculation Of Chemical Reaction Rates For Polyatomics. *Comput. Phys. Commun.* **1992**, *71*, 235−262.
(46) Liu, Y. P.; Lynch, G. C.; Truong, T. N.; Lu, D. H.; Truhlar, D. G.; Garrett, B. C. Molecular Modeling Of The Kinetic Isotope Effect For The [1,5]-Sigmatropic Rearrangement Of Cis-1,3-Pentadiene. *J. Am. Chem. Soc.* **1993**, *115*, 2408−2415.
(47) Zheng, J.; Zhang, S.; Lynch, B. J.; Corchado, J. C.; Chuang, Y. -Y.; Fast, P. L.; Hu, W.-P.; Liu, Y.-P.; Lynch, G. C.; Nguyen, K. A.; et al. *POLYRATE*, version 2008; University of Minnesota: Minneapolis, MN, 2009.
(48) Zheng, J.; Zhang, S.; Corchado, J. C.; Chuang, Y.-Y.; Coitiño, E. L.; Ellingson, B. A.; Truhlar, D. G. *GAUSSRATE*, version 2009-A; University of Minnesota: Minneapolis, MN, 2010.
(49) Chase, M. W., Jr. NIST-JANAF Thermochemical Tables, 4th ed. *J. Phys. Chem. Ref. Data, Monogr.* **1998**, *9*, 1298.
(50) Ragains, M. L.; Finlayson-Pitts, B. J. Kinetics and Mechanism of the Reaction of Cl Atoms with 2-Methyl-1,3-butadiene (Isoprene) at 298 K. *J. Phys. Chem. A* **1997**, *101*, 1509−1517.
(51) Coquet, S.; Ariya, P. A. Kinetics of the Gas-Phase Reactions of Cl Atom with Selected C_2−C_5 Unsaturated Hydrocarbons at 283 < T < 323 K. *Int. J. Chem. Kinet.* **2000**, *32*, 478−484; Erratum: "Kinetics of the Gas-Phase Reactions of Cl Atom with Selected C2−C5 Unsaturated Hydrocarbons at 283 < T < 323 K," Int. J. Chem. Kinet. 2000, 32, 478. *Int. J. Chem. Kinet.* **2010**, *42*, 692.
(52) Ahmed, M.; Blunt, D.; Chen, D.; Suits, A. G. UV Photodissociation of Oxalyl Chloride Yields Four Fragments from One Photon Absorption. *J. Chem. Phys.* **1997**, *106*, 7617.
(53) Tyndall, G. S.; Orlando, J. J.; Kegley-Owen, C. S. Rate Coefficients for Quenching of C1 ($2P_{1/2}$) by Various Atmospheric Gases. *J. Chem. Soc., Faraday Trans.* **1995**, *91*, 3055.
(54) Choi, N.; Pilling, M. J.; Seakins, P. W.; Wang, L. Studies of Site Selective Hydrogen Atom Abstractions by Cl Atoms from Isobutane and Propane by Laser Flash Photolysis/IR Diode Laser Spectroscopy. *Phys. Chem. Chem. Phys.* **2006**, *8*, 2172.
(55) http://pubchem.ncbi.nlm.nih.gov/compound/p-cymene#section=3D-Conformer.

DOI: 10.1021/jp509800g
J. Phys. Chem. A 2015, 119, 559−570

(56) Chuang, Y.-Y.; Corchado, J. C.; Truhlar, D. G. Mapped Interpolation Scheme for Single-Point Energy Corrections in Reaction Rate Calculations and a Critical Evaluation of Dual-Level Reaction Path Dynamics Methods. *J. Phys. Chem. A* **1999**, *103*, 1140−1149.
(57) Wallington, T. J.; Skewes, L. M.; Siegl, W. O. Kinetics of the Gas-Phase Reaction of Chlorine Atoms with A Series of Alkenes, Alkynes and Aromatic Species at 295 K. *J. Photochem. Photobiol., A* **1988**, *45*, 167−175.
(58) Shi, J.; Bernhard, M. J. Kinetic Studies of the Cl-Atom Reactions with Selected Aromatic Compounds Using the Photochemical Reactor-FTIR Spectroscopy Technique. *Int. J. Chem. Kinet.* **1997**, *29*, 349−358.
(59) Anderson, R. S.; Huang, L.; Iannone, R.; Rudolph, J. Laboratory Measurements of the $^{12}C/^{13}C$ Kinetic Isotope Effects in the Gas-Phase Reactions of Unsaturated Hydrocarbons with Cl Atoms at 298 ± 3 K. *J. Atmos. Chem.* **2007**, *56*, 275−291.
(60) Atkinson, R.; Aschmann, S. M. Kinetics of the Gas-Phase Reaction of Cl Atoms with a Series of Organics at 296 ± 2 K and Atmospheric Pressure. *Int. J. Chem. Kinet.* **1985**, *17*, 33−41.
(61) Bartels, M.; Edelbuttel-Einhaus, J.; Hoyermann, K. The Reactions of Benzyl Radicals with Hydrogen Atoms, Oxygen Atoms, and Molecular Oxygen Using EI/REMPI Mass Spectrometry. *Symp. (Int.) Combust., [Proc.]* **1989**, *22*, 1041−1051.
(62) Markert, F.; Pagsberg, P. UV Spectra and Kinetics of Radicals Produced in the Gas Phase Reactions of Cl, F and OH with Toluene. *Chem. Phys. Lett.* **1993**, *209*, 445−454.
(63) Nozière, B.; Lesclaux, R.; Hurley, M. D.; Dearth, M. A.; Wallington, T. J. A Kinetic and Mechanistic Study of the Self-Reaction and Reaction with HO_2 of the Benzylperoxy Radical. *J. Phys. Chem.* **1994**, *98*, 2864−2873.
(64) Fantechi, G.; Jensen, N. R.; Saastad, O.; Hjorth, J.; Peeters, J. Reactions of Cl Atoms with Selected VOCs: Kinetics, Products and Mechanisms. *J. Atmos. Chem.* **1998**, *31*, 247−267.
(65) Wang, L.; Arey, J.; Atkinson, R. Reactions of Chlorine Atoms with a Series of Aromatic Hydrocarbons. *Environ. Sci. Technol.* **2005**, *39*, 5302−5310.
(66) Prinn, R.; Weiss, R.; Millar, B.; Jaung, J.; Alyea, F.; Cunnold, D.; Fraser, P.; Hartley, D.; Simmonds, P. Atmospheric Trends and Lifetime of CH_3CCI_3 and Global OH Concentrations. *Science* **1995**, *269*, 187−192.
(67) Atkinson, R. Atmospheric Chemistry of VOCs and NOx. *Atmos. Environ.* **2000**, *34*, 2063−2101.

DOI: 10.1021/jp509800g
J. Phys. Chem. A 2015, 119, 559−570